

Acoustic Mode Frequencies of the Sun during the Minimum Phase between Solar Cycles 23 and 24

S. C. Tripathy · K. Jain · F. Hill

© Springer

Abstract We investigate the spatial and temporal variations of the high-degree mode frequencies calculated over localized regions of the Sun during the extended minimum phase between solar cycles 23 and 24. The frequency shifts measured relative to the spatial average over the solar disk indicate that the correlation between the frequency shift and magnetic field strength during the low-activity phase is weak. The disk-averaged frequency shifts computed relative to a minimal activity period also reveal a moderate correlation with different activity indices, with a maximum linear correlation of about 72%. From the investigation of the frequency shifts at different latitudinal bands, we do not find a consensus period for the onset of solar cycle 24. The frequency shifts corresponding to most of the latitudes in the northern hemisphere and 30° south of the equator indicate the minimum epoch to be February 2008, which is earlier than inferred from solar activity indices.

Keywords: Data analysis; Helioseismology; Solar cycle

1. Introduction

The analysis of continuous helioseismic data over solar cycle 23 has produced many interesting results related to the cyclic variation of the oscillation frequencies and other mode parameters. Most of the studies are confined to the low- and intermediate-degree modes (Jain, Tripathy, and Hill, 2011; and references therein) which reinforces the idea that the mode frequencies change with solar activity level. However, the period of extended minimum between cycles 23 and 24 produced some surprises, most notably a disagreement between the low- and intermediate-degree modes regarding the onset of cycle 24. Based on data from the Global Oscillation at Low Frequency (GOLF) instrument on-board the *Solar and Heliospheric Observatory* (SOHO), Salabert *et al.* (2009) pointed out that cycle 24 started in late 2007. This was later substantiated by the analysis of Birmingham Solar Oscillation Network (BiSON) data (Fletcher *et al.*, 2010). But the analysis of intermediate-degree mode frequencies from Global Oscillation

¹ National Solar Observatory, Tucson, AZ 85719, USA
email: stripathy@nso.edu email: kjain@nso.edu email: fhill@nso.edu

Network Group (GONG) and Michelson Doppler Imager (MDI) did not confirm the early onset (Jain *et al.*, 2010). Instead the occurrence of the minimum was shown to be around the middle of 2008 for MDI data and the end of 2008 for GONG data (Tripathy *et al.*, 2010b). The latter period approximately coincided with the minimum period observed in solar activity indices. A more detailed investigation of low- and intermediate-degree modes from GONG data, to eliminate the instrument dependence, demonstrated that the extended minimum period as seen in oscillation frequencies consist of two minima depending on the degree of the modes. The frequencies when analyzed as a function of the latitude also showed two minima at high latitude in contrast to a single minimum at mid-low latitudes (Jain, Tripathy, and Hill, 2011).

In the context of the extended minimum, we present here results obtained from the analysis of the high-degree mode frequencies in the degree range of $180 \leq \ell \leq 1000$ obtained using a technique of local helioseismology. With the use of a limited data set during the ascending phase of the solar cycle, Hindman *et al.* (2000) have explored the behavior of such high-degree modes and noted that the frequency variations are spatially as well as temporally associated with active regions. The analysis of high-degree global modes (Rhodes, Reiter, and Schou, 2002) showed that the frequency shifts of p -modes changed sign from positive to negative at frequencies near the acoustic cut-off and confirmed the earlier results obtained from the analysis of intermediate-degree modes (Ronan, Cadorna, and Labonte, 1994; Jefferies, 1998). The higher frequencies of the high-degree modes were further found to be anti-correlated with solar activity (Rhodes, Reiter, and Schou, 2003; Rose *et al.*, 2003). In the context of local helioseismology, Howe *et al.* (2008) studied frequencies of high-degree modes over localized regions of the Sun and found that the frequencies of modes beyond the acoustic cutoff have negative correlation with the local surface magnetic-field strength. The analysis of modes $\ell \leq 1000$ obtained from the global analysis during 1996–2008 (Rhodes *et al.*, 2011) not only confirmed the earlier results but also indicated a further reversal around the frequency of approximately $6950 \mu\text{Hz}$ *i.e.* the frequencies were found to be positively correlated with the changes in activity indices. This investigation also pointed out that the frequencies where these reversals occur change with the mean level of activity. Rabello-Soares (2011) has also investigated the properties of the globally determined intermediate and high-degree modes ($20 \leq \ell \leq 900$) from MDI and reports evidence of a quadratic relation between the frequency shifts and 10.7 cm radio flux, $F_{10.7}$.

Since the high-degree global oscillation modes cannot distinguish between the northern and southern hemispheres and are longitudinally averaged, we use the high-degree modes obtained through the ring-diagram technique to examine their behavior at different latitudes during the extended minimum phase and to record the onset time of solar cycle 24. We also explore the correlation between the frequency shifts and the strength of the magnetic activity during this phase. Preliminary results from a similar investigation but involving only a few Carrington rotations were reported by Tripathy, Jain, and Hill (2010a, 2011). The correlation analysis is further extended to include other activity indices, *viz.* $F_{10.7}$ and the international sunspot number R_i .

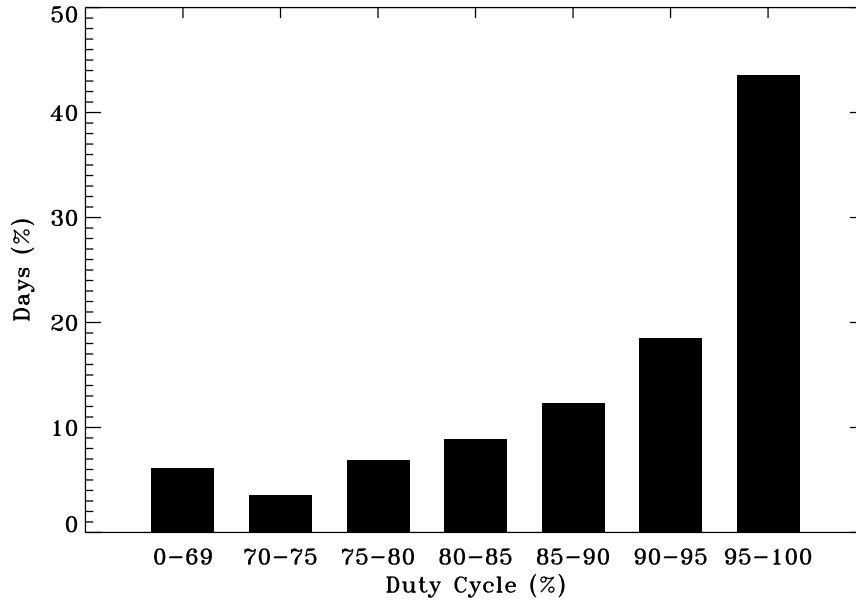


Figure 1. Distribution of the duty cycle of GONG ring-data between 26 April 2007 and 7 August 2010.

2. Data and Analysis

We use the ring-diagram technique (Hill, 1988) to calculate the high-degree mode frequencies in the range of $180 \leq \ell \leq 1000$ and examine the spatial as well as temporal frequency shifts during the extended minimum phase covering Carrington rotations (CR) 2056 to 2099 starting with 26 April 2007 and ending with 7 August 2010. The mode frequencies corresponding to the 189 dense-pack overlapping tiles are extracted from the GONG website <http://gong.nso.edu>. Each region covers an area of $16^\circ \times 16^\circ$ in heliographic latitude and longitude and is tracked for a period of 1664 min (hereinafter one ring-day) using a model solar velocity (Snodgrass, 1984). The centers of the regions are separated by 7.5° in latitude and longitude and extend to roughly 52.5° from the disk center, covering a substantial portion of the solar disk. On the time domain, successive ring days are overlapped between 27 and 30 min. Each tracked region is then apodized with a circular function and converted to a three-dimensional power spectra by applying a FFT in both spatial and temporal directions (Corbard *et al.*, 2003). The resulting power spectra are fitted with a Lorentzian profile model to obtain the mode parameters (Haber *et al.*, 2000). The effective duty cycle of the data considered here ranges from 32% to 100% with a mean of about 90%. Figure 1 shows the distribution of duty cycle. For this analysis, we included only data for which the duty cycle exceeds 70%, which yielded usable data for 991 out of 1056 ring-days and close to 180000 individual tiles.

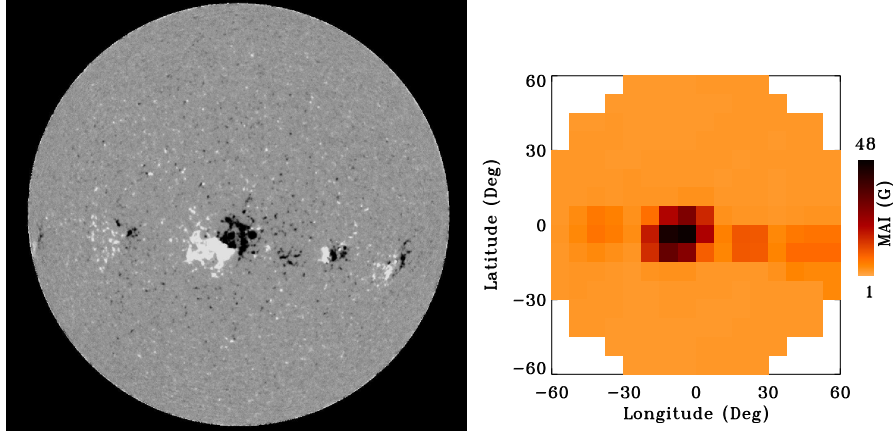


Figure 2. GONG full-disk magnetogram taken at 13:57:16 UT, corresponding to the mid-time of the ring-day of 7 June 2007, is shown in the left panel. The MAI map of the same ring-day covering $\pm 60^\circ$ in latitude and longitude is shown in the right panel.

We also determine the level of local magnetic activity associated with each tile by calculating a magnetic activity index (MAI) from the GONG magnetograms. In this study, we use magnetograms sampled every 32 min, mapped and tracked in the same way as the Dopplergrams. The remapped values are subjected to the same spatial apodization used in preparing the Doppler power spectra, so that both of them have the identical spatial extent. All of the pixels, with a field strength higher than 2.5 times the noise level of a given pixel in GONG magnetograms, are then averaged to represent the MAI of the tile. Figure 2 shows an example of the full-disk GONG magnetogram and the corresponding MAI map covering $\pm 60^\circ$ in latitude and longitude for the ring-day 7 June 2007. The correspondence between the two is easily visible in the figure.

It has been shown earlier that the mode parameters measured by the ring-diagram analysis are influenced by the foreshortening. There has also been evidence that the duty cycle of the observation introduces bias in the measured quantities. Therefore, it is necessary to correct the frequencies for the duty cycle and geometric effects. Following Howe *et al.* (2004a), we model the effects of position of the disk as a two-dimensional function of the distance from the disk center ρ without the cross-terms, combined with a linear dependence on the duty cycle $f(t)$ of the observations,

$$\nu(\rho_x, \rho_y, t) = a_0 + a_1\rho_x + a_2\rho_x^2 + a_3\rho_y + a_4\rho_y^2 + a_5f(t) \quad (1)$$

where ρ_x and ρ_y are the longitudinal and latitudinal component of ρ , and a_i are coefficients determined by fitting. In order to minimize the effect of the magnetic field on the fitting, we use the frequencies over a two year quiet period between 1 September 2007 and 31 August 2009 and evaluated the a_i s for each (n, ℓ) mode. The corrected frequency of each mode is then used for the analysis. Figure 3 illustrates the variations of the coefficients as a function of frequency. The linear terms are an order of magnitude smaller than the quadratic terms,

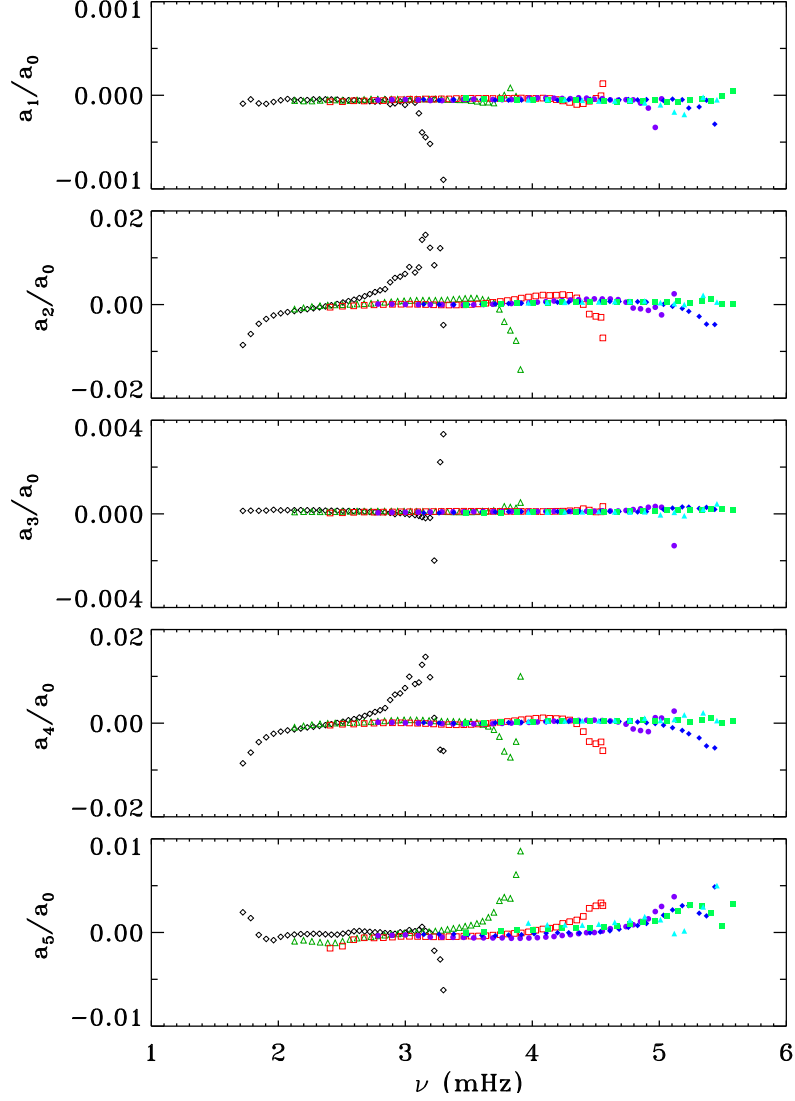


Figure 3. Coefficients of the quadratic fit of frequencies to the distance from the disk center and the duty cycle, divided by the constant term a_0 . The symbols denote different n values: open diamond: $n = 0$, open triangle: $n = 1$, open square: $n = 2$, filled circle: $n = 3$, filled diamond: $n = 4$, filled square: $n = 5$, and filled triangle: $n = 6$.

but not insignificant. Figure 4 shows an example of the frequency differences at the extreme disk position within the 189 tiles located at a latitude of 52.5° north of the equator and 22.5° west of central meridian corresponding to 10 June 2008.

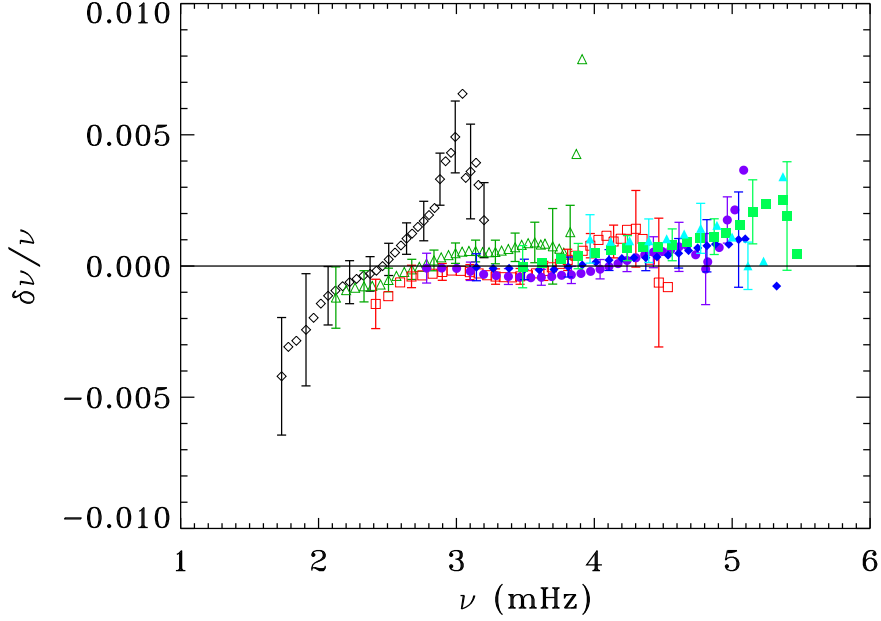


Figure 4. Frequency differences between the corrected and fitted frequencies for a tile centered at a latitude of 52.5° north of the equator and 22.5° west of central meridian as a function of frequency. Errors for every third point are only shown. The symbols denote different n values: open diamond: $n = 0$, open triangle: $n = 1$, open square: $n = 2$, filled circle: $n = 3$, filled diamond: $n = 4$, filled square: $n = 5$, and filled triangle: $n = 6$.

3. Results and Discussions

3.1. Spatial Variation

In order to explore the spatial variation of the frequencies and its correlation with the MAI of the corresponding tile, we calculate a mean spatial frequency shift for each ring-day. First, the frequency difference of each mode ($\delta\nu_{n,\ell}$) is calculated with respect to a reference frequency which is the error-weighted average of that particular mode present in 189 dense-pack tiles. This difference is then averaged, weighted by the mean error, over all the modes present in the tile to estimate the spatial frequency shift ($\delta\nu_s$) one value for each tile according to

$$\delta\nu_s = \sum_{n,\ell} \frac{\delta\nu_{n,\ell}}{\sigma_{n,\ell}^2} / \sum_{n,\ell} \frac{1}{\sigma_{n,\ell}^2}. \quad (2)$$

As noted in Hindman *et al.* (2000), the mean frequency shifts would have been zero but for the presence of activity on the solar disk. Examples of the frequency shifts and coeval MAIs over 189 tiles for two different phases of the solar cycle 23 are presented by Tripathy, Jain, and Hill (2011). Here we concentrate on Pearson's linear correlation coefficient (r_p) obtained between 189 $\delta\nu_s$ and MAI for each ring-day. The resultant correlation coefficients as a function of the mean

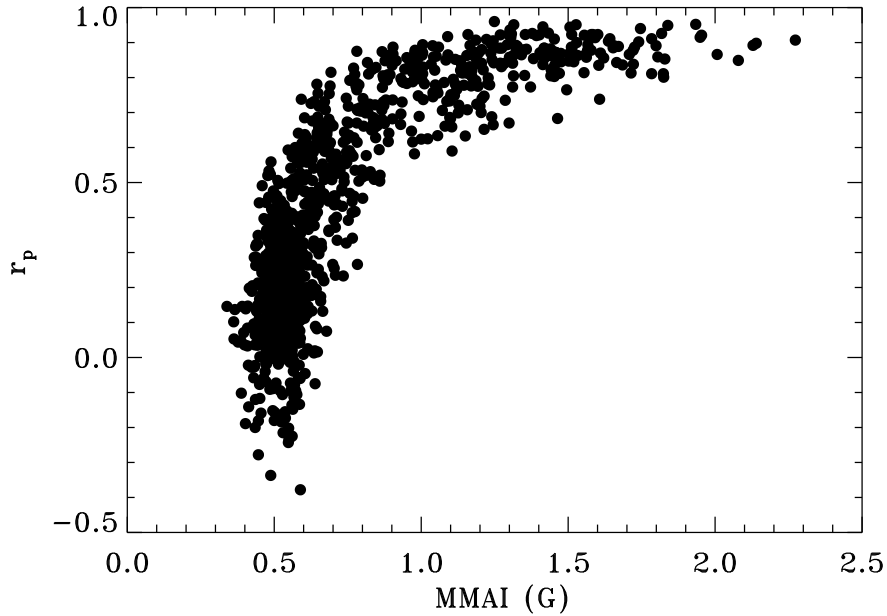


Figure 5. Linear correlation coefficient r_p between the measurement of $\delta\nu_s$ and MAI of 189 tiles for 991 ring-days.

magnetic activity index (MMAI) for 991 ring-days are shown in Figure 5, where MMAI is the mean MAI over the 189 dense-pack tiles. As shown in earlier studies, mostly confined to active regions (Rajaguru, Basu, and Antia, 2001) or high-activity periods (Howe *et al.*, 2004b), the shifts, in general, have a higher correlation at higher MAIs. However, Figure 5 indicates that tiles with small MAIs do not correlate well with the shifts, indicating that the frequency shifts act as a tracer of magnetic field only if the MMAI is above a threshold value. We also notice that during the lowest activity period, $\delta\nu$ is anti-correlated with MMAI. Although the values of the coefficients are not significant, it is worth mentioning that a similar result for the low- (Salabert *et al.*, 2009) and intermediate-degree (Tripathy *et al.*, 2010b) global-mode frequencies have been reported earlier.

3.2. Temporal Variation

Figure 6 displays the temporal evolution of MMAI and indicates that the extended minimum phase in solar activity occurred between 2007 and 2010 with the deepest phase lasting for one year between mid-2008 and mid-2009. In order to eliminate the random fluctuations produced by daily variations, we calculate a 23-point running mean that approximately corresponds to an average over a Carrington rotation period. This is shown by the solid line in the figure. Although, most of the random fluctuations are reduced, we still notice rises and dips throughout the minimum phase. These fluctuations have been interpreted as a quasi-biennial signal in global low-degree modes (Fletcher *et al.*, 2010) and its origin is suspected to be near the shear layer just beneath the surface.

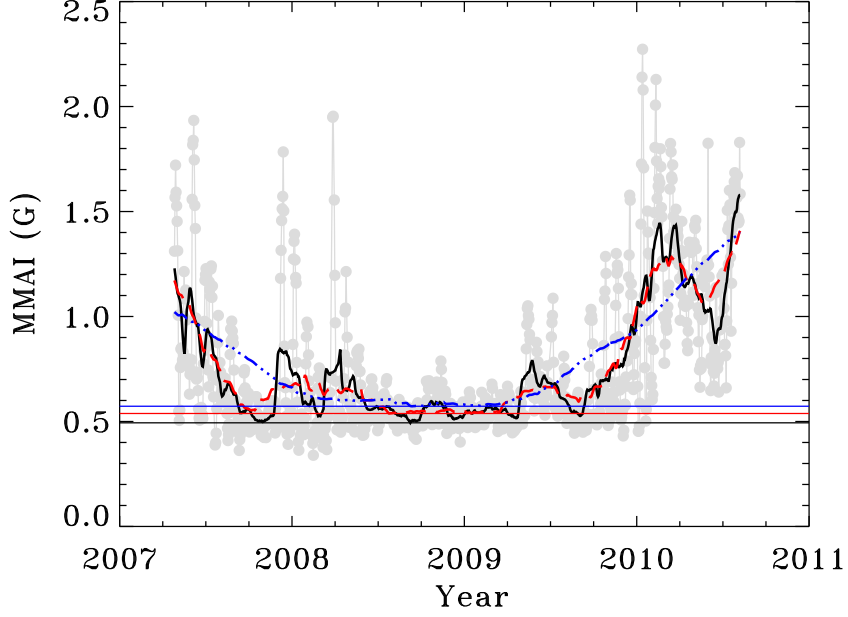


Figure 6. Temporal evolution of mean magnetic activity index (MMAI). The black (solid), red (dashed) and blue (dashed-dot-dot-dot) lines represent the running mean over 23, 91, and 365 points. The horizontal lines indicate the position of the minimum epochs.

From the smoothed data, it is easy to estimate the epoch of the solar minimum which is defined as the lowest value in the data set and found to be around September 2008 in agreement with the epoch of the minimum associated with other activity indices. However, a value of similar magnitude as the minimum seen during September 2008 is also noticed during the third quarter of 2007, hinting at the possibility of existence of a double minimum. To test if the position of the minimum changes with the number of points used for smoothing, we additionally smooth the data with 91 (dashed line) and 365 (dash-dot-dot-dot line) points and find that the position of the minimum does not change significantly. Except for the data smoothed with 365 points, which probably represents over-smoothing, we find the signature of double minima in MMAI, the 2007 period coinciding with the minimum epoch inferred from the analysis of the low-degree modes (Salabert *et al.*, 2009) and the 2008 period with intermediate-degree modes (Tripathy *et al.*, 2010b).

In order to characterize the temporal evolution of the mode frequencies, we calculate the mean frequency shift ($\delta\nu$) using a formula which is analogous to the frequency shifts calculated for the global modes,

$$\delta\nu = \sum_{n,\ell} \frac{\sum_{i=1}^{189} \delta\nu_{n,\ell}(t)}{\sigma_{n,\ell}^2} / \sum_{n,\ell} \frac{1}{\sigma_{n,\ell}^2}, \quad (3)$$

Table 1. Pearson linear (r_p) and Spearman rank (r_s) correlation statistics between $\delta\nu$ and activity indices. The calculated probabilities of having null correlations in each case are smaller than 10^{-10} .

Activity	r_p		r_s	
	Raw	Smooth	Raw	Smooth
MMAI	0.52	0.72	0.50	0.66
$F_{10.7}$	0.41	0.68	0.36	0.58
R_I	0.39	0.65	0.38	0.57

where $\delta\nu_{n,\ell}$ is the frequency difference with respect to the frequencies corresponding to the ring-day of 11 May 2008. Since $\delta\nu$ represents the frequency shift over a large area of the solar disk and covers the activity belt, we consider these shifts to represent global shifts over each ring-day.

The temporal variation of the calculated $\delta\nu$ and the associated running mean over 23 points is shown in Figure 7. As before, we use the lowest value in smoothed frequency shifts to calculate the epoch of the solar minimum. It is evident that the minimum occurred in February 2008, roughly in agreement with the emergence of a sunspot group with the polarities of the new cycle during January 2008. However the appearance of several sunspots at low latitudes with cycle 23 polarities a few months later indicated otherwise (Phillips, 2008). Furthermore, the minimum seen in frequency shifts does not agree with the minimum epoch observed in MMAI hinting at a weak correlation between them.

Since $\delta\nu$ represents disk-averaged quantity, we can further compute their relation with other global activity indices. In Figure 7, we show the temporal variation of the international sunspot number (R_I) and 10.7 cm radio flux ($F_{10.7}$) interpolated to the same temporal grid of frequency shifts. The linear correlation coefficient between $\delta\nu$ and different activity indices is presented in Table 1. It is evident that the smoothed correlation is significantly higher than the raw correlation but in no case does the value exceed 72% implying at best a moderate correlation. As expected, the correlation is higher between $\delta\nu$ and MMAI since these are calculated locally over the same tile while the other two indices reflect global measurements over the entire solar disk.

3.3. Temporal Variation over CR

We further investigate the temporal variation of the frequency shifts for each CR separately, where the frequency difference of each multiplet ($\delta\nu_{n,\ell}(t)$) is calculated by subtracting an average frequency over the entire CR for each disk position. This difference is used in Equation (3) to calculate the shift for each ring-day. It may be noted that not all CRs include a uniform set of 24 ring-days since the data have been weeded for low duty-cycle values. Figure 8 shows the rank correlation coefficients between the frequency shifts and MMAI as a function of time (top panel) and MMAI (bottom panel). In the top panel, the

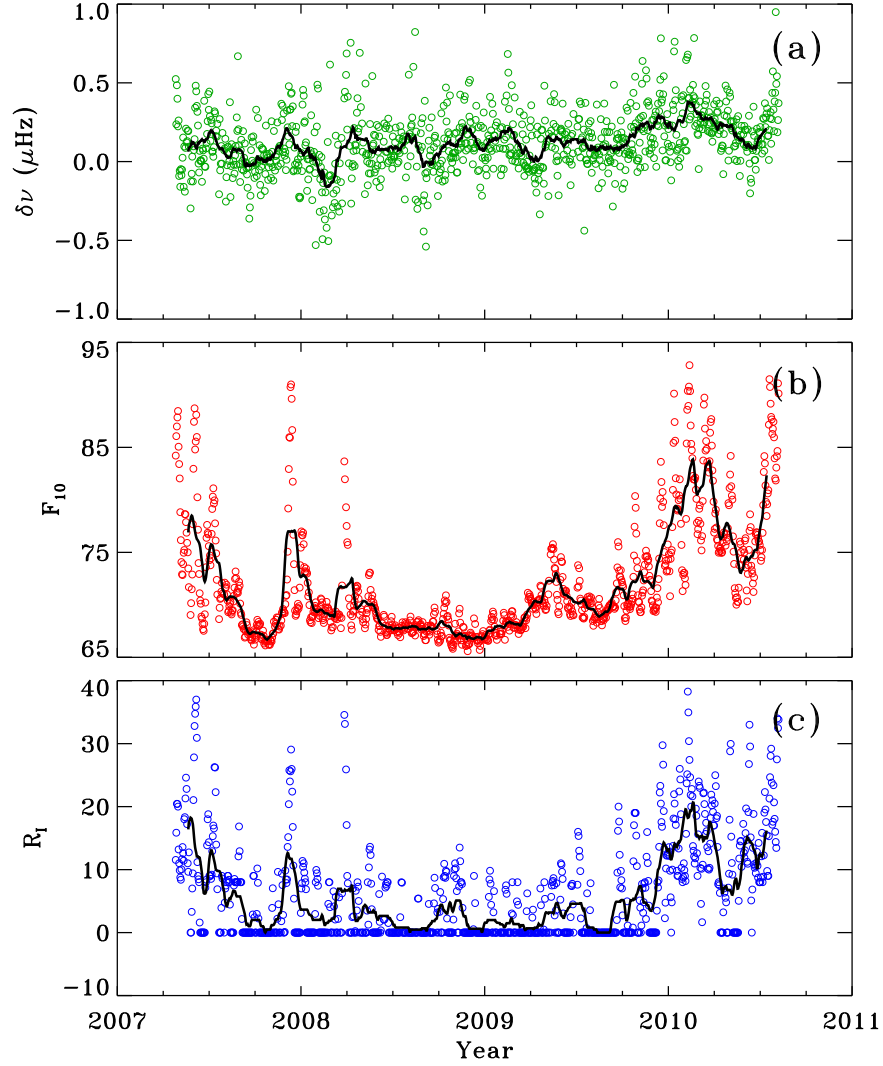


Figure 7. Temporal evolution of (a) $\delta\nu$, (b) $F_{10.7}$, and (c) R_I . The solid black line in each panel represents the running mean over 23 points.

filled (open) symbols refer to those values where the two-sided significance is smaller (larger) than 0.1 indicating significant (weak) correlation, respectively. Thus, the negative and few positive correlation coefficients with values less than about 0.5, shown by open symbols, are not significant. From the bottom panel, where all the coefficients are shown by filled symbols, it is evident that with the increase of MAI, the magnitude of the correlation coefficient slowly increases.

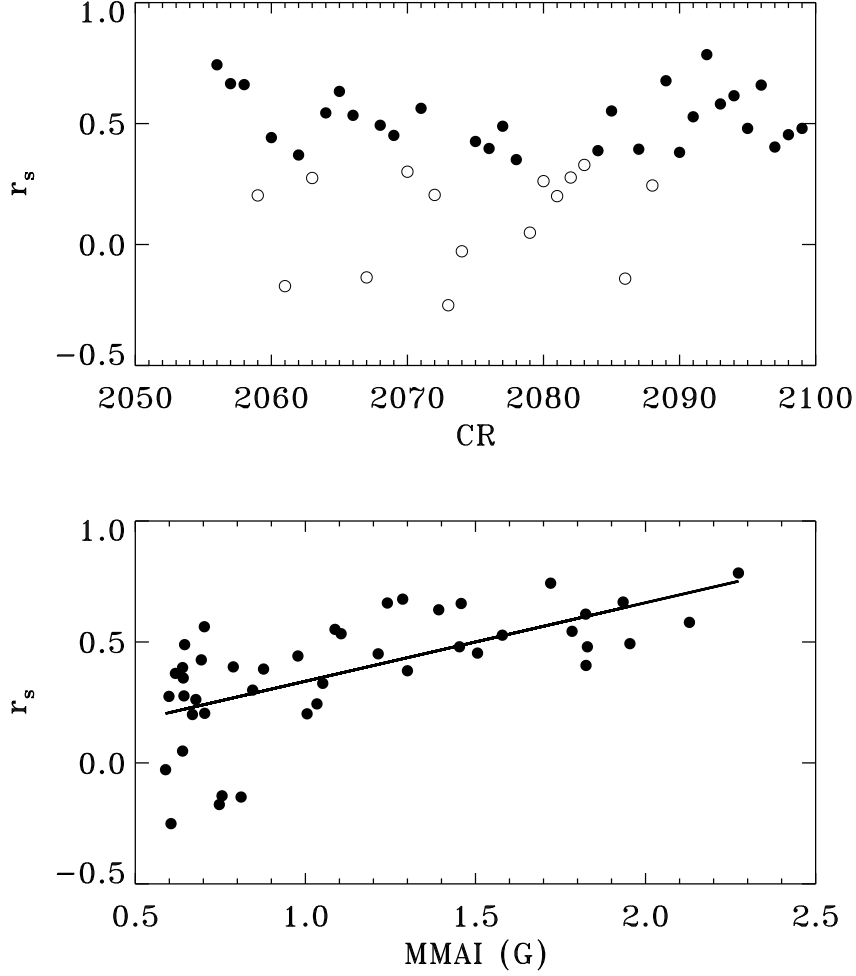


Figure 8. Rank correlation coefficient (r_s) between the frequency shifts and MMAI calculated for each ring-day and sampled over each CR (top panel) for different CRs and (b) as a function of MMAI. The filled (open) circles in the top panel represent the values where the two-sided significance is smaller (larger) than 0.1, respectively, whereas in the bottom panel all the coefficients are shown by filled circles. The solid line in the bottom panel represents the linear fit.

However, the rank correlation between MMAI and r_s is about 65% again implying a weak correlation. The variations in the rank correlation coefficients shown here are similar to Pearson’s linear correlation coefficients shown in Figure 4 of Tripathy, Jain, and Hill (2011) except for CR 2081. However, the values of the coefficients for the overlapping CRs between the two analyses cannot be compared since they represent coefficients calculated from two different correlation methods.

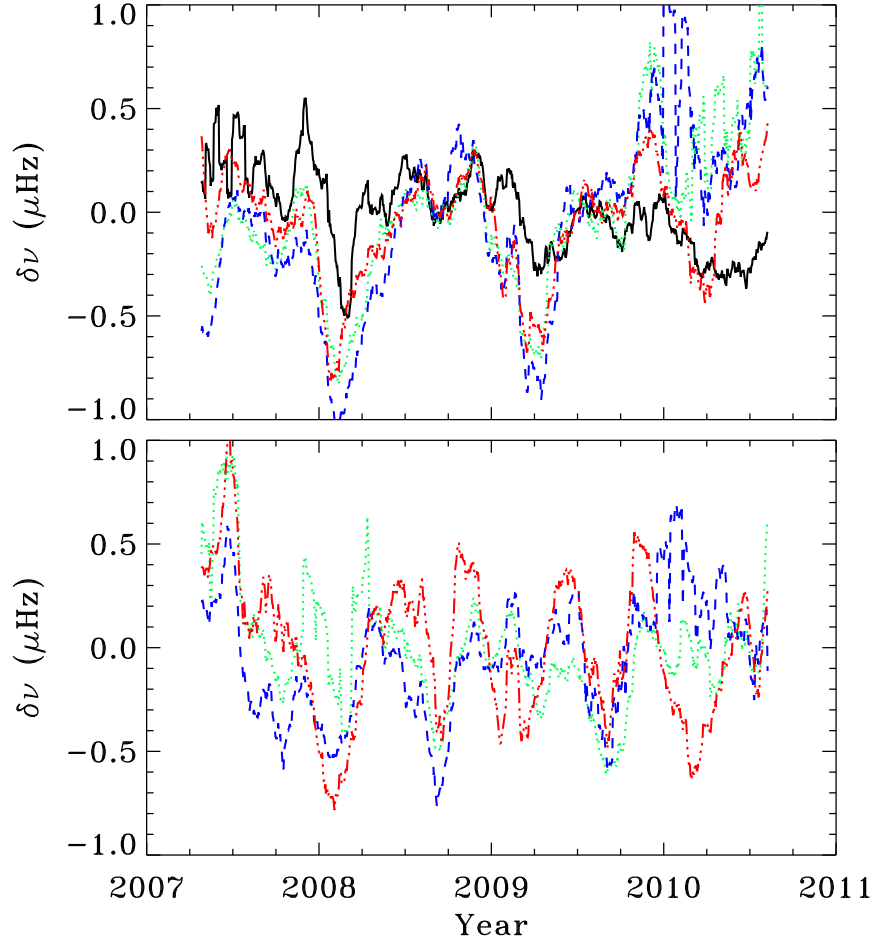


Figure 9. Temporal variation of frequency shifts as a running mean over 23 points at selected latitudes on the central meridian; latitudes north of the equator including the equator (top panel) and latitudes south of the equator (bottom panel). Line styles have the following meaning: black (solid): equator, green (dotted): 15° , blue (dashed): 30° , and red (dash-three-dots): 45° .

3.4. Latitudinal Variation

As mentioned earlier, there is no consensus regarding the epoch of the solar minimum based on the helioseismic data. Recent analysis of the global frequency shifts also indicates the possible existence of one or two minima at different latitudes (Jain, Tripathy, and Hill, 2011). In order to find out if the mode frequencies calculated locally follow latitudinal patterns similar to global modes, we use Equation (3) to calculate frequency shifts ($\delta\nu_{\text{lat}}$) for different latitudes located on the central meridian. Here $\delta\nu_{n,\ell}$ is calculated with respect

to an average frequency at the given latitude on the central meridian over all the ring-days. The running mean over 23 points of the resultant frequency shifts for selected latitudes is displayed in Figure 9. In the northern hemisphere (Figure 9 (top)), the signature of the minimum can be clearly seen at two different epochs, the first minimum around February 2008 and the second around the first quarter of 2009. In case of the equator, we also notice a third dip around the middle of 2010 where the shifts are marginally smaller compared to the dip in 2009. In the southern hemisphere, the picture is less clear as we notice many dips associated with each of the curve. This may be a consequence of the fact that during cycle 23, the southern hemisphere was more active compared to the northern hemisphere. As a result even a small amount of activity in the southern hemisphere would influence the mode frequencies and as a consequence our calculation of minimum based on the lowest value in the smoothed frequencies may not be the appropriate method. However, if we stick to this definition of the lowest value as the representation of the solar minimum, we find that the minimum in frequency shifts at 15° , 30° , and 45° south of the equator is around September 2009, September 2008, and February 2008, respectively. In order to understand how closely $\delta\nu_{\text{lat}}$ follows the magnetic activity at different latitudinal bands, we compute Pearson's linear and Spearman's rank correlation coefficients between $\delta\nu_{\text{lat}}$ and MAI of the tiles of the same latitude used for the calculation of frequency shifts. These coefficients along with the position of the minimum epoch for all latitude bands is given in Table 2. It is clear that the frequency shifts corresponding to different latitudes in the northern and southern hemisphere point to different epochs of the solar minimum with varying degree of correlation. In the equator and northern hemisphere, $\delta\nu_{\text{lat}}$ of all the latitude bands except for the one located at 37.5° indicate a minimum around February 2008 while in the southern hemisphere we do not have a consistent epoch of the minimum period, the significant deviation is seen in the tiles located at latitudes of 7.5° and 15° south of the equator. If we consider only those latitudes for which the correlation between $\delta\nu_{\text{lat}}$ and MAI is approximately 80%, then we find that 50% of the latitudes indicate the epoch of the minimum to be around February 2008 which is consistent with the frequency shifts measured over the entire disk but earlier than inferred from MMAI and other solar activity indicators. We also notice a small negative coefficient for the tiles located at 52.5° south of the equator but the anti-correlation is not significant due to the low value of the correlation coefficient. Finally we note that the signature of the onset of solar cycle 24 as early as the third quarter of 2007 is not found in this analysis.

4. Summary

Using the ring-diagram technique applied to GONG data, we have examined the behavior of the high-degree modes during the extended minimum phase between cycles 23 and 24. Since the mode parameters measured by the ring-diagram technique are subject to foreshortening and duty cycle effects, we modeled the effect of the position of the disk as a two-dimensional function of the distance from the disk center combined with a linear dependence of the duty cycle and find that the correction factor is not significant in the 3 mHz band.

Table 2. Pearson linear (r_p) and Spearman rank (r_s) correlation statistics at different latitudes between $\delta\nu_{\text{lat}}$ and corresponding MAI and the time of occurrence of the minimum frequency shift.

Latitude	r_p	r_s	Minimum epoch
52.5°	0.08	0.09	February 2008
45.0°	0.37	0.29	February 2008
37.5°	0.63	0.40	March 2009
30.0°	0.88	0.51	February 2008
22.5°	0.85	0.57	February 2008
15.0°	0.83	0.43	February 2008
7.5°	0.57	0.32	February 2008
0.0°	0.78	0.45	February 2008
−7.5°	0.94	0.52	April 2010
−15.0°	0.85	0.49	August 2009
−22.5°	0.80	0.43	September 2008
−30.0°	0.79	0.38	September 2008
−37.5°	0.49	0.20	February 2008
−45.0°	0.04	0.02	February 2008
−52.5°	− 0.16	− 0.17	February 2008

Since it has been argued by Hindman *et al.* (2000) that active regions are responsible for the global-frequency shifts, we estimate the equivalent of a global frequency shift by computing an average over the local frequency shifts over the regions covered in dense-pack analysis. These shifts appear to be of the order of 1 μHz during the minimum activity phase as opposed to 3 μHz in the 3-mHz band in the 1998 MDI data deduced by Hindman *et al.* (2000). This discrepancy may be attributed to the level of magnetic activity during the two periods.

We have also investigated the epoch of the minimum phase as seen in the oscillation frequencies and find that the disk-averaged frequency shift indicates a minimum around February 2008 roughly in agreement with the emergence of a sunspot group with the polarities of the new cycle. However, the times of minimum inferred from different latitudes do not, in general, agree with each other. While the minimum at different latitudes in the northern hemisphere mostly agree the minimum to be around February 2008 with a lead time of about six months to the activity indicators, the minimum in the southern hemisphere shows a consistent time of February 2008 only for latitudes higher than 30° south of the equator where there is little or no activity. If we consider only those latitudes for which the correlation between $\delta\nu_{\text{lat}}$ and MAI is approximately 80%, then we find that 50% of the latitudes indicate the epoch of the minimum to be around February 2008 consistent with the frequency shifts measured over the entire disk.

Since the magnetic-field strength of the Sun during the period of extended minimum phase is dominated by the quiet-sun magnetic field, we find that both the spatial and temporal shifts are weakly correlated with the surface magnetic activity. On this basis, we argue that the shifts can-not be accounted for by the

regions of observed component of the magnetic field alone but may be explained as a combined effect of the magnetic field and temperature changes (Kuhn, 2001) or as an effect of a change in the acoustic cavity size (Dziembowski and Goode, 2005). The exact mechanism for these changes still remains an open question.

Acknowledgements We thank the reviewer for useful comments. This work utilizes data obtained by the Global Oscillation Network Group (GONG) program, managed by the National Solar Observatory, which is operated by AURA, Inc. under a cooperative agreement with the National Science Foundation. The data were acquired by instruments operated by the Big Bear Solar Observatory, High Altitude Observatory, Learmonth Solar Observatory, Udaipur Solar Observatory, Instituto de Astrofísica de Canarias, and Cerro Tololo Interamerican Observatory. This work is partially supported by NASA grants NNG05HL41I and NNG08EI54I to the National Solar Observatory.

References

- Corbard, T., Toner, C., Hill, F., Hanna, K.D., Haber, D.A., Hindman, B.W., Bogart, R.S.: 2003, Ring-diagram analysis with GONG++. In: Sawaya-Lacoste, H. (ed.) *GONG+ 2002. Local and Global Helioseismology: the Present and Future*, ESA SP-517, 255.
- Dziembowski, W.A., Goode, P.R.: 2005, Sources of oscillation frequency increase with rising solar activity. *Astrophys. J.* **625**, 548.
- Fletcher, S., New, R., Broomhall, A.M., Chaplin, W., Elsworth, Y.: 2010, The new solar minimum: How deep does the problem go? In: Cranmer, S. R., Hoeksema, J. T., Kohl, J. L. (eds.) *SOHO-23: Understanding a Peculiar Solar Minimum*, ASP Conf. Ser. **428**, 43.
- Haber, D.A., Hindman, B.W., Toomre, J., Bogart, R.S., Thompson, M.J., Hill, F.: 2000, Solar shear flows deduced from helioseismic dense-pack samplings of ring diagrams. *Solar Phys.* **192**, 335.
- Hill, F.: 1988, Rings and trumpets - Three-dimensional power spectra of solar oscillations. *Astrophys. J.* **333**, 996.
- Hindman, B., Haber, D., Toomre, J., Bogart, R.: 2000, Local fractional frequency shifts used as tracers of magnetic activity. *Solar Phys.* **192**, 363.
- Howe, R., Komm, R.W., Hill, F., Haber, D.A., Hindman, B.W.: 2004a, Activity-related changes in local solar acoustic mode parameters from Michelson Doppler Imager and Global Oscillations Network Group. *Astrophys. J.* **608**, 562.
- Howe, R., Komm, R.W., González Hernández, I., Hill, F., Haber, D.A., Hindman, B.W.: 2004b, Local Frequency Shifts from GONG and MDI. In: Danesy, D. (ed.) *SOHO 14 Helio- and Asteroseismology: Towards a Golden Future*, ESA SP-559, 484.
- Howe, R., Haber, D.A., Hindman, B.W., Komm, R., Hill, F., Gonzalez Hernandez, I.: 2008, Helioseismic frequency shifts in active regions. In: Howe, R., Komm, R. W., Balasubramaniam, K. S., Petrie, G. J. D. (eds.) *Subsurface and Atmospheric Influences on Solar Activity*, ASP Conf. Ser. **383**, 305.
- Jain, K., Tripathy, S.C., Hill, F.: 2011, How peculiar was the recent extended minimum: A hint toward double minima. *Astrophys. J.* **739**, 6.
- Jain, K., Tripathy, S.C., Burtseva, O., González-Hernández, I., Hill, F., Howe, R., Kholikov, S., Komm, R., Leibacher, J.: 2010, What solar oscillation tell us about the solar minimum. In: Cranmer, S. R., Hoeksema, J. T., Kohl, J. L. (eds.) *SOHO-23: Understanding a Peculiar Solar Minimum*, ASP Conf. Ser. **428**, 57.
- Jefferies, S.M.: 1998, High-frequency (pseudo-) modes. In: Deubner, F. L., Christensen-Dalsgaard, J., Kurtz, D. (eds.) *New Eyes to See Inside the Sun and Stars*, IAU Symp. **185**, 415.
- Kuhn, J.R.: 2001, One solar cycle later: reflections and speculations on directions in helio- and asteroseismology in a new millennium. In: Wilson, A., Pallé, P. L. (eds.) *SOHO 10/GONG 2000 Workshop: Helio- and Asteroseismology at the Dawn of the Millennium*, ESA SP-464, 7.

-
- Phillips, T.: 2008, Old solar cycle returns. *NASA Science News*, http://science.nasa.gov/science-news/science-at-nasa/2008/28mar_oldcycle/.
- Rabello-Soares, M.C.: 2011, Characterization of solar-cycle induced frequency shift of medium- and high-degree acoustic modes. *J. Phys. Conf. Ser.* **271**, 012026.
- Rajaguru, S.P., Basu, S., Antia, H.M.: 2001, Ring diagram analysis of the characteristics of solar oscillation modes in active regions. *Astrophys. J.* **563**, 410.
- Rhodes, E.J. Jr., Reiter, J., Schou, J.: 2002, Solar cycle variability of high-frequency and high-degree p-mode oscillation frequencies. In: Wilson, A. (ed.) *From Solar Min to Max: Half a Solar Cycle with SOHO*, ESA SP-508, 37.
- Rhodes, E.J. Jr., Reiter, J., Schou, J.: 2003, High-degree p-modes and the sun's evolving surface. In: Sawaya-Lacoste, H. (ed.) *GONG+ 2002. Local and Global Helioseismology: the Present and Future*, ESA SP-517, 173.
- Rhodes, E.J., Reiter, J., Schou, J., Larson, T., Scherrer, P., Brooks, J., McFaddin, P., Miller, B., Rodriguez, J., Yoo, J.: 2011, Temporal changes in the frequencies of the solar p-mode oscillations during solar cycle 23. In: Choudhary, D.P., Strassmeier, K.G. (eds.) *Physics of Sun and Star Spots*, IAU Symp. **273**, 389.
- Ronan, R.S., Cadorna, K., Labonte, B.J.: 1994, Solar cycle changes in the high frequency spectrum. *Solar Phys.* **150**, 389.
- Rose, P., Rhodes, E.J. Jr., Reiter, J., Rudnisky, W.: 2003, Studies of the sensitivity of p-mode oscillation frequencies to changing levels of solar activity. In: Sawaya-Lacoste, H. (ed.) *GONG+ 2002. Local and Global Helioseismology: the Present and Future*, ESA SP-517, 373.
- Salabert, D., García, R.A., Pallé, P.L., Jiménez-Reyes, S.J.: 2009, The onset of solar cycle 24. What global acoustic modes are telling us. *Astron. Astrophys.* **504**, L1.
- Snodgrass, H.B.: 1984, Separation of large-scale photospheric Doppler patterns. *Solar Phys.* **94**, 13.
- Tripathy, S.C., Jain, K., Hill, F.: 2010a, Do active regions modify oscillation frequencies? In: Hasan, S. S., Rutten, R. J. (eds.) *Magnetic Coupling between the Interior and Atmosphere of the Sun*, Springer, Berlin. 374.
- Tripathy, S.C., Jain, K., Hill, F.: 2011, Variation of high-degree mode frequencies during the declining phase of solar cycle 23. *J. Phys. Conf. Ser.* **271**, 012024.
- Tripathy, S.C., Jain, K., Hill, F., Leibacher, J.W.: 2010b, Unusual trends in solar p-mode frequencies during the current extended minimum. *Astrophys. J. Lett.* **711**, L84.